Vision Research 238 (2026) 108720

Contents lists available at ScienceDirect

Vision Research

journal homepage: www.elsevier.com/locate/visres

Visual discomfort for flickering sinusoids is not predicted by the spatio-temporal contrast sensitivity function☆

Paul B. Hibbard [a,b,*], Jordi M. Asher [a,b], Louise O'Hare [c], Caitlin Evans [a], Caelan Dow [a]

[a] University of Stirling, Department of Psychology, Stirling, FK9 4LA, Scotland, UK
[b] University of Essex, Department of Psychology, Wivenhoe Park, Colchester, CO4 3SQ, Essex, UK
[c] Nottingham Trent University, Department of Psychology, 50 Shakespeare Street, Nottingham, NG1 4FQ, Nottinghamshire, UK

ARTICLE INFO

Keywords:
Visual discomfort
Spatial frequency
Temporal frequency
Contrast sensitivity
Sensory sensitivity

ABSTRACT

Visual discomfort, the unpleasant, aversive experience associated with some visual stimuli, is most pronounced for flickering and spatially repetitive stimuli. It has been proposed that the degree of visual discomfort for such stimuli can be predicted by the contrast sensitivity function, peaking at midrange spatial and temporal frequencies. We evaluated the spatio-temporal tuning of visual discomfort for flickering, sinusoidal stimuli. Discomfort increased with spatial frequency for static and slowly flickering stimuli, but decreased with spatial frequency for stimuli flickering at 16 Hz. Discomfort increased with temporal frequency for spatially uniform stimuli, and for all spatial frequencies. Flickering stimuli were more uncomfortable than static stimuli of any spatial frequency. Spatially uniform stimuli flickering at 16 Hz, the highest frequency tested, were rated as the most uncomfortable. These results deviate from the contrast sensitivity function, which predicts that discomfort should be highest for static stimuli, with bandpass spatial frequency tuning. This discrepancy indicates that threshold-level visual sensitivity is not a good predictor of visual discomfort for high contrast stimuli. Our results are however consistent with efficient coding models, which predict higher levels of excitation for high spatial and temporal frequencies when stimuli are presented at a high contrast. They are also consistent with physiological measures of cortical responses to high contrast stimuli.

1. Introduction

1.1. Visual discomfort

Visual discomfort refers to the unpleasant and aversive perceptual experience evoked by certain visual patterns. This experience may be accompanied by other symptoms, such as eye strain, headache, dry eyes, diplopia, illusory motion (shimmering and scintillating) or illusory colours (Conlon et al., 1999; Evans & Stevenson, 2008). While some people are subject to heightened subjective visual sensitivity (Kurczewska et al., 2024; Price et al., 2025a; Ward, 2019), visual discomfort is something that is experienced across the population as a whole. The current study is primarily concerned with the stimulus parameters that are associated with visual discomfort, rather than the individual differences that lead to increased sensitivity to this phenomenon in some people.

A broad range of stimuli are associated with visual discomfort, and can be characterised across four key dimensions: brightness, spatially repeating patterns, temporal flicker, and intense visual environments (Price et al., 2025b). It has been hypothesised that discomfort occurs when stimuli deviate from natural scene statistics in a way that leads to hyperexcitation of the visual cortex (Haigh et al., 2013; Hibbard & O'Hare, 2015; Penacchio et al., 2023; Wilkins, 1995; Wilkins & Hibbard, 2014). Under this interpretation, spatially repetitive and flickering stimuli are uncomfortable as they are uncommon in nature, and create large electrophysiological and haemodynamic responses (Gentile & Aguirre, 2020; Huang et al., 2003, 2011; Orekhova et al., 2019).

1.2. Visual discomfort, contrast sensitivity and cortical activity

Here, we outline the contrast sensitivity function (CSF) and its relevance to visual discomfort, as it has been proposed that the stimulus properties influencing discomfort reflect the CSF (Fernandez & Wilkins, 2008). This function describes the sensitivity of the visual system to different combinations of spatial and temporal frequency, in terms of the minimum contrast required to detect the presence of a stimulus (Robson, 1966). For static stimuli, contrast sensitivity is bandpass, with a peak around 2–5 cycles per degree, and decreases for both lower and higher frequencies. For stimuli flickering above approximately 8 Hz

☆ This article is part of a Special issue entitled: 'Sensory discomfort' published in Vision Research.

* Corresponding author at: University of Stirling, Department of Psychology, Stirling, FK9 4LA, Scotland, UK.
E-mail address: paul.hibbard@stirling.ac.uk (P.B. Hibbard).

https://doi.org/10.1016/j.visres.2025.108720
Received 22 August 2025; Received in revised form 31 October 2025; Accepted 11 November 2025
Available online 14 November 2025

contrast sensitivity tends to be low-pass, such that sensitivity does not vary between low and midrange spatial frequencies, and decreases only for high spatial frequencies. Similarly, the temporal frequency tuning of contrast sensitivity is bandpass for low spatial frequencies, with peak sensitivity at 8–10 Hz. For spatial frequencies above 1–2 cycles/degree temporal contrast sensitivity is lowpass, with sensitivity decreasing for frequencies above 10 Hz. This non-separable spatio-temporal frequency tuning, in which the spatial frequency tuning of contrast sensitivity depends on temporal frequency and *vice versa*, is illustrated in Figs. 1–2. This joint tuning to spatial and temporal frequency reflects the combined responses of the magnocellular and parvocellular processing streams, which are most responsive to spatially coarse, rapidly changing stimuli, and static, fine-detailed stimuli, respectively (Legge, 1978; Schiller & Logothetis, 1990).

The CSF describes our ability to detect stimuli at low contrast, rather than the high contrast stimuli more typically associated with visual discomfort (Yoshimoto et al., 2017). However, the cortical activity evoked by visual stimuli shows similar spatio-temporal tuning. Stimuli with a midrange spatial frequency, around 3–5 cycles degree, produce the largest visually evoked potentials (Tyler et al., 1979). In the temporal domain, the greatest evoked potentials for full-field flicker are generated for stimuli around 10 Hz (Regan, 1989). For sinusoidal gratings, the amplitude of VEPs also depends on spatial and temporal frequency. The greatest responses are evoked by combinations of low spatial frequency and high temporal frequency, or high spatial frequency and low temporal frequency (Regan, 1978; Tyler et al., 1978).

1.3. Spatial frequency tuning of visual discomfort

Some psychophysical studies of the effect of spatial frequency on discomfort have provided evidence consistent with the idea that the degree of discomfort reflects contrast sensitivity. Wilkins et al. (1984) found that rated pleasantness was lowest for square-wave gratings with a spatial frequency of 4 cycles/degree, and that the number of illusions and adverse somatic effects (such as eye strain, headache or dizziness) was also highest for this frequency. Fernandez and Wilkins (2008) found that natural images and abstract artworks that were associated with discomfort tended to have greater contrast amplitude for intermediate spatial frequencies, around 3 cycles per degree. Random noise that has been filtered to have an excess energy in midrange frequencies has also been found to be more uncomfortable (Fernandez & Wilkins, 2008), with a peak in discomfort for frequencies between 0.375 and 1.5 cycles per degree (O'Hare & Hibbard, 2011).

Other studies however have found that visual discomfort increases with spatial frequency, rather than being maximum for a value close to the peak of the CSF. Conlon et al. (2001) found that somatic difficulty and perceptual distortion increased with spatial frequency between 1 and 16 cycles/degree for squarewave gratings. Evans and Stevenson (2008) found that pattern glare, a measure of the perceptual distortions associated with visual discomfort, was lowest for low frequency squarewave stimuli (0.5 cycles/degree), but did not differ between midrange (3.0 cycles/degree) and high (12 cycles/degree) frequencies. Monger et al. (2016) found that perceptual distortions and discomfort increased with spatial frequency using 0.3, 2.3 and 9.4 cycles/degree squarewave gratings. Visual discomfort has also been found to *decrease* with increasing spatial frequency between 0.5 and 9 cycles/degree for retinally-stabilised sinusoidal grating stimuli (O'Hare et al., 2015).

The spatial frequency tuning of visual discomfort is also subject to individual differences associated with increased sensory sensitivity. Conlon et al. (2001) showed that perceptual distortions and somatic difficulty increased with spatial frequency between 1 and 12 cycles/degree for a group with low sensitivity to discomfort, but peaked at 4–8 cycles/degree for a high-sensitivity group. Shepherd et al. (2013) compared responses to squarewave gratings between migraine and control groups. While spatial frequency did not affect discomfort, for the control group the number of illusions was greatest at 3 cycles/degree, and was lower at 12 cycles/degree. In contrast, for the migraine group the number of illusions was highest for both the 3 cycles/degree and 12 cycles/degree groups. Wilson et al. (2015) measured pattern glare for square-wave gratings of 0.3, 2.3 and 9.4 cycles/degree in myalgic encephalomyelitis (ME). They found that pattern glare increased with spatial frequency for the control group, but was consistently high for both mid and high spatial frequency gratings for the ME group. Overall, previous research does not show a consistent spatial frequency profile for discomfort, with findings ranging from CSF-like peaks to steady increases or decreases depending on stimulus type, population and task.

1.4. Temporal frequency tuning of visual discomfort

The relationship between temporal frequency and visual discomfort is also inconsistent across studies. Some have found peaks in discomfort that align with predictions from the CSF, whereas others have observed different temporal tuning patterns. For example, Gentile and Aguirre (2020) measured discomfort for large, spatially uniform stimuli that flickered sinusoidally. For luminance flicker, discomfort peaked at 18.6 Hz, and there was a strong correlation between discomfort ratings and SSVEP amplitude. O'Hare (2017) found that, for sinusoidal gratings flickering at 5 or 10 Hz, visual discomfort decreased with spatial frequency from 0.4 to 9 cycles/degree, as was also found for static stimuli (O'Hare et al., 2015). In contrast O'Hare and Hibbard (2024) found that, for sinusoidal gratings flickering at 5 Hz, discomfort was lowest when the spatial frequency was 3 cycles/degree, increasing for both lower and higher spatial frequencies. Ogawa and Motoyoshi (2021) found that the unpleasantness of spatiotemporally bandpass filtered noise peaked at 0.5–2 Hz, and this temporal frequency tuning was much sharper for spatially narrowband stimuli. Yoshimoto et al. (2017) measured discomfort for square-wave spatial stimuli flickering at 1 Hz. For square-wave and sawtooth temporal waveforms, discomfort increased when the amplitude spectrum deviated from a 1/f amplitude profile. For randomised waveforms, discomfort was greatest when there was an increase in amplitude around 15 Hz, or when the slope of the amplitude spectrum was decreased, shifting the amplitude spectrum towards higher temporal frequencies. The effects of temporal frequency thus vary significantly with the stimulus type (spatially uniform versus bandpass noise stimuli) and the task (discomfort versus unpleasantness ratings).

1.5. Stimulus size and eccentricity

Visual discomfort is affected by the size and location of stimuli, as well as their spatial and temporal frequency spectra. If discomfort is related to the degree of cortical activity, then increasing the size of a stimulus should increase the level of discomfort. This prediction needs to take account of the cortical magnification factor, which describes how central visual stimuli are mapped to a greater area of the visual cortex than more peripheral ones. Central visual stimuli evoke greater neural activity, and are thus predicted to evoke more discomfort than peripheral ones, when stimulus size is matched. Consistent with this Wilkins et al. (1984) found that, when comparing central and peripheral targets, paroxysmal activity in EEG recordings and the number of illusions reported were better predicted by the area of cortex each stimulus would activate, than by the size of the stimulus itself.

The location of a stimulus in the visual field might also be expected to influence the effects of spatial and temporal frequency on discomfort. This is because the contrast sensitivity function is affected by eccentricity, with peak sensitivity shifting to lower spatial frequencies, and higher temporal frequencies, away from the fovea. This shift is consistent with the increasing importance of the magnocellular system with increasing eccentricity (Masri et al., 2020).

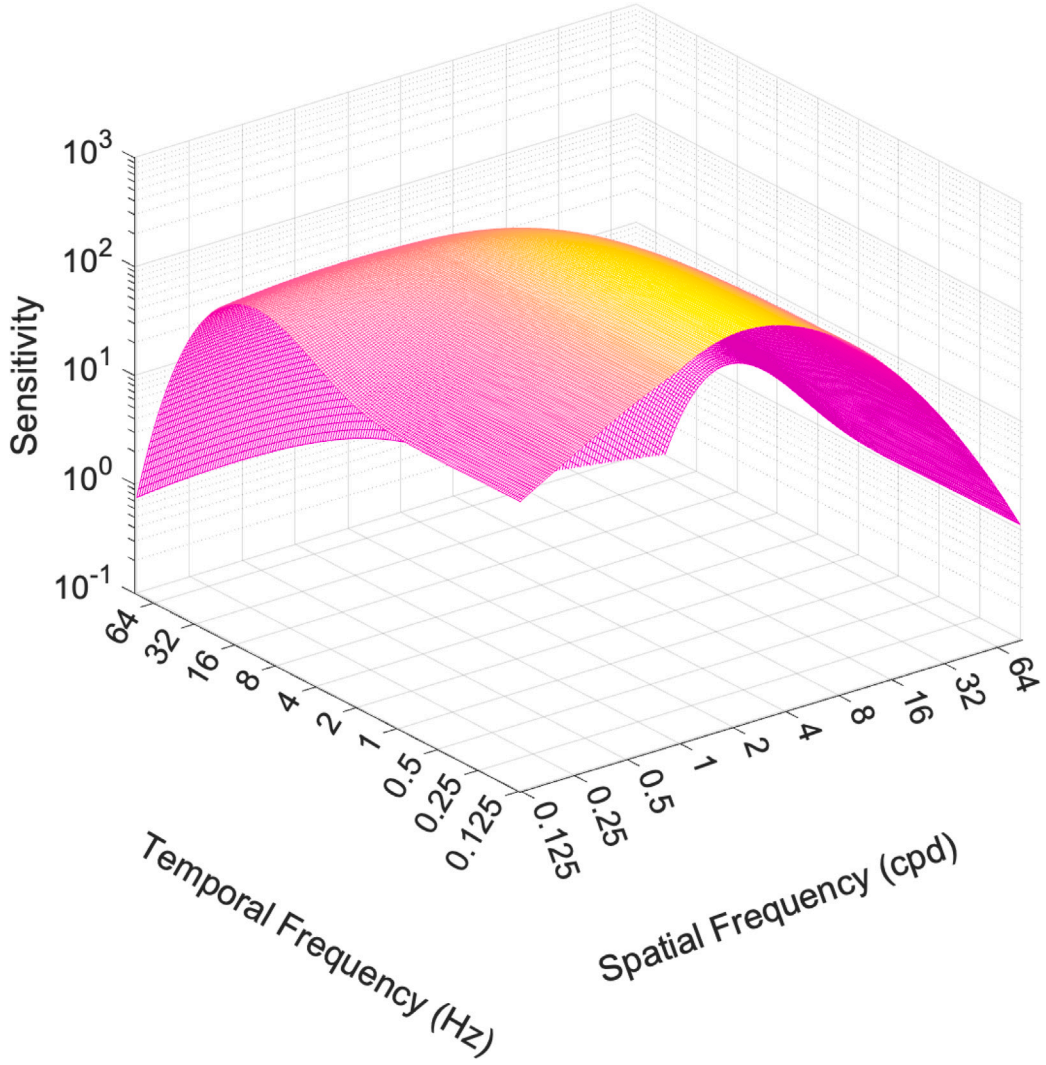

Fig. 1. The contrast sensitivity function, which describes the sensitivity of the visual system to the presence of visual patterns, varies with both spatial and temporal frequency. This function was created using the castleCSF model of contrast sensitivity (Ashraf et al., 2024), using stimulus parameters corresponding to our centrally presented circular stimuli (see methods for full stimulus details).

The visual field may be divided into foveal and extrafoveal regions. While the transition between these regions is smooth, Strasburger et al. (2011) describes the central 5° as foveal, between 5–9° as parafoveal and 9–17° as perifoveal, and these three regions together form the macula. Many investigations of visual discomfort, including the Pattern Glare Test, have tended to present stimuli within this macular region, subtending between 10 and 15° (Conlon et al., 2001; Evans & Stevenson, 2008; Wilkins et al., 1984).

1.6. Rationale and hypotheses for the present study

The aim of the current study was to measure how visual discomfort for narrowband sinusoidal stimuli varies with both spatial and temporal frequency. While both parameters are important determinants of visual discomfort, a full spatio-temporal tuning profile is not currently available. As well as providing a characterisation of how discomfort varies with both spatial and temporal frequency, it also allows us to evaluate the idea that this will reflect the CSF. If so, then it is predicted that, for static stimuli and those with a low flicker rate, discomfort will be maximal around 2–5 cycles/degree, reducing for both lower and higher frequencies. For faster flicker rates, visual discomfort is predicted to be highest for low spatial frequencies, and to reduce above 4 cycles/degree. For flickering stimuli, discomfort is predicted to be highest around 8–10 Hz for unpatterned and low-spatial frequency stimuli, reducing for higher and lower rates of flicker. For higher spatial frequencies, discomfort is predicted to be highest at low temporal frequencies, and to reduce above 10 Hz. We also measured visual discomfort for both central and more peripheral stimuli, since the CSF varies with eccentricity. Specifically, peak contrast sensitivity shifts to lower spatial frequencies, and higher temporal frequencies, away from the fovea.

In summary, visual discomfort is shaped by both the spatial and temporal properties of visual stimuli, yet previous findings show mixed patterns that often diverge from predictions based on the contrast sensitivity function. The present study examines discomfort across a comprehensive range of spatial and temporal frequencies, in both central and more peripheral vision, to test whether these patterns follow CSF-like tuning, with particular focus on the effects of introducing flicker.

2. Methods

2.1. Participants

23 participants completed the study (mean age 24, 15 female). The study and procedures were approved by the University of Stirling General University Ethics Panel (GUEP 2024 18703 14535).

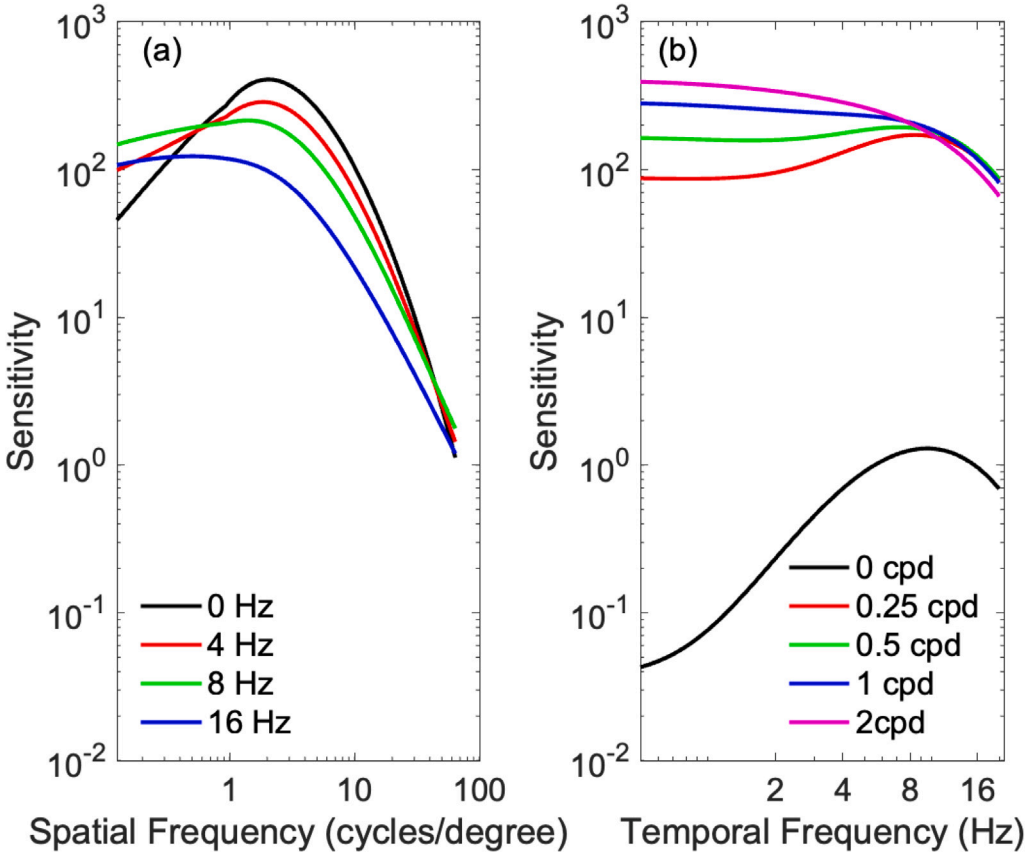

Fig. 2. The contrast sensitivity function shown in Fig. 1 plotted to show spatial and temporal tuning separately. (a) For static stimuli, or those flickering at 4 Hz or less, the CSF is bandpass, with a peak around 4 cycles/degree. For stimuli with a higher rate of flicker, contrast sensitivity is lowpass, with contrast sensitivity constant at low spatial frequencies, and reducing for spatial frequencies above 4 cycles/degree. (b) For flickering stimuli, contrast sensitivity is bandpass when the stimulus has a low spatial frequency, with sensitivity peaking around 10 Hz. For higher spatial frequencies, the function is lowpass, with sensitivity constant for low rates of flicker, and reducing above 10 Hz. Sensitivity is highest overall for static stimuli with a spatial frequency of 2 cycles/degree. These functions were created using the castleCSF model of contrast sensitivity (Ashraf et al., 2024), using stimulus parameters corresponding to our centrally presented circular stimuli (see methods for full stimulus details).

2.2. Apparatus

Stimuli were presented on a VIEWPixx/3D monitor (1920 × 1080 resolution; 52.5 cm × 29.5 cm screen size; 120 Hz refresh rate) controlled by MATLAB R2025a. Stimulus presentation was controlled using MATLAB 2025a and Psychtoolbox extensions (Brainard et al., 2024; Kleiner et al., 2007) on a Windows 10 PC. At a viewing distance of 62 cm, each pixel subtended 1.52 arc min of visual angle. The display operated in 10-bit greyscale mode. High-precision timing and stimulus synchronisation were managed using a VPixx DataPixx3. Participants' responses were collected via a standard keyboard, and head position was stabilised using a chin rest throughout the experiment.

2.3. Materials

Stimuli in all conditions consisted of vertical sinusoidal luminance gratings presented in greyscale on a uniform mid-grey background. Gratings varied in spatial frequency (0, 0.5, 1, 2, 4, or 8 cycles/degree) and temporal frequency (0, 1, 2, 4, 8, or 16 Hz). Temporal modulation was implemented via cosine-phase contrast reversals at the specified temporal frequency to create counterphase flicker. All stimuli were presented with a Michelson contrast of 0.8 with a mean luminance of 100 cd m^{-2}. All 25 combinations of non-zero spatial and temporal frequencies were presented. In addition, static stimuli (0 Hz) at all 5 spatial frequencies, and spatially uniform, unpatterned stimuli (0 cycles/degree) at all 5 temporal frequencies were also presented.

Each grating was created using one of three spatial windows. In the circle condition, the stimulus was visible within a centrally presented circular aperture with a diameter of 10.1°. In the small-annulus condition, the stimulus occupied an annular region extending from 10.1° to 14.3° in diameter, centred on fixation. In the large-annulus condition, the stimulus was shown in an annular region extending from 10.1° to 20.2° in diameter. The circle and small-annulus stimuli were matched for stimulus area, whereas the width of the annulus in the large-annulus condition matched the radius of the stimulus in the central condition. All stimuli fell broadly within the macular area, being neither confined to the fovea and parafovea, nor extending to truly peripheral locations beyond 30° (Strasburger et al., 2011) (see Fig. 3).

A red fixation cross was continuously present throughout the task, centred on the screen. Each arm of the cross was 40 pixels in length, corresponding to approximately 1.0° of visual angle .

2.4. Procedure

After providing informed consent, participants completed a 9-item Leiden Visual Sensitivity Scale (Perenboom et al., 2018) assessing self-reported sensitivity to sunlight, artificial light, flicker, patterned stimuli, and after-effects. Ratings were made using a continuous on-screen slider scale from 'not at all' to 'very'. Responses to each question were scaled linearly between 0–4 so that the total score ranged between 0 and 36, for direct comparison with other studies.

The experiment was conducted in a dark room where participants completed three experimental blocks corresponding to the three spatial

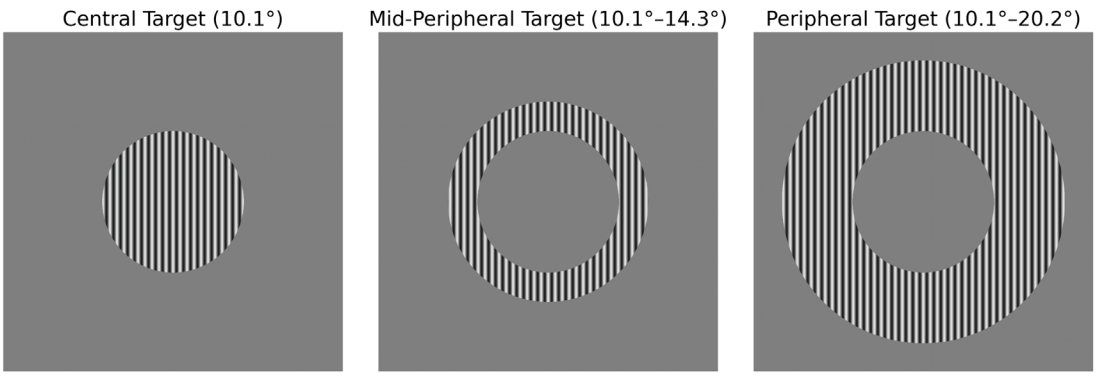

Fig. 3. Examples of sinusoidal grating stimuli used in the experiment. Stimuli were vertical sinusoids varying in both spatial frequency (0–8 cycles/degree) and temporal frequency (0–16 Hz), implemented as counterphase contrast reversals. Stimuli were presented within one of three spatial masks: (Left) central circular aperture (10.1° diameter), (Centre) small-annulus (10.1°–14.3°), and (Right) large-annulus (10.1°–20.2°). Gratings were displayed on a mid-grey background and overlaid with a red fixation cross.

target conditions (circle, small-annulus, large-annulus), with both block order and trial order randomised separately for each participant. Each block comprised 35 trials, or 105 trials in total. On each trial, a stimulus with a given spatial and temporal frequency was presented for 2 s, and participants rated its discomfort using an on-screen slider, where the scale was internally coded from 0 to 1 (with higher values indicating greater discomfort). Participants were instructed to interpret 'discomfort' in the context of the Leiden Visual Sensitivity Scale, which includes questions on the extent to which they are bothered by flicker and patterned stimuli.

The fixation cross remained visible throughout the experiment. Brief on-screen instructions were presented between blocks, and participants initiated each block with a keypress. The full session, including questionnaire and experimental trials, lasted approximately 25–30 min.

3. Results

3.1. Spatial frequency tuning for static sinusoidal stimuli

Results for static sinusoidal stimuli are shown in Fig. 4a. In all cases, discomfort ratings are plotted alongside predicted contrast sensitivity for direct comparison. For all three stimulus configurations, discomfort increased with spatial frequency across the full range tested (0.5–8 cycles/degree). In comparison with flickering stimuli (Fig. 4c), the degree of discomfort was relatively modest, with mean ratings ranging between 0.19 and 0.35. Discomfort is reported on the 0–1 scale described in the Methods, where 0 corresponds to the minimum and 1 to the maximum discomfort rating.

Data were analysed with a linear mixed effects model, with stimulus configuration (C) as a categorical predictor and the log of spatial frequency (f) as a linear predictor, including a random intercept for each participant: `discomfort ~ C * log(f) + (1 | Participant)`. Discomfort ratings increased with the spatial frequency of the pattern (t(339) = 3.0, p = 0.03), but were not affected by stimulus configuration (circle versus small annulus: t(339) = 0.75, p = 0.45; circle versus large annulus:t(339) = 1.46, p = 0.14), and there was no interaction between the two (small-annulus x f: t(339) = 0.45, p = 0.65; large-annulus x f: t(339) = 0.031, p = 0.98).

3.2. Temporal frequency tuning for flickering spatially uniform stimuli

Results for the flickering spatially uniform stimuli are shown in Fig. 4c. For all three stimulus configurations, discomfort increased with temporal frequency across the full range tested (1–16 Hz). In comparison with static stimuli, flicker was much more uncomfortable, with mean ratings ranging between 0.37 and 0.85.

Data were analysed with a linear mixed effects model, with stimulus configuration (C) as a categorical predictor and the log of temporal frequency (ω) as a linear predictor, including a random intercept for each participant: `discomfort ~ C * log(ω) + (1 | Participant)`. Discomfort ratings increased with the temporal frequency of flicker (t(339) = 12.5, $p < .001$), but were not affected by stimulus configuration (circle versus small-annulus: t(339) = 1.0, p = 0.32; circle versus large-annulus: t(339) = 1.51, p = 0.13) and there was no interaction between the two (small-annulus x ω: t(339) = −0.91, p = 0.36; small-annulus x ω: t(339) = −0.77, p = 0.44).

3.3. Spatio-temporal frequency tuning for flickering sinusoidal stimuli

Results for flickering sinusoidal gratings are shown in Figs. 5–7 for the three stimulus configurations. In each case, data are plotted as a function of both spatial and temporal frequency. As for static gratings, visual discomfort tended to increase with increasing spatial frequency for most flicker rates. Visual discomfort also increased with temporal frequency.

Data were analysed with a linear mixed effects model, with stimulus configuration as a categorical predictor, and log(spatial frequency) and log(temporal frequency) as linear predictors: `discomfort ~ C * log(f) * log(ω) + (1 | Participant)`.

Visual discomfort increased with spatial (t(1713)=5.12, p< .001) and temporal (t(1713)=15.0, p< .001) frequency, and was higher for the large annulus (t(1713) = 3.7, p< .001). There was an interaction between the effects of configuration and spatial and temporal frequency. The overall increase in discomfort ratings for both annulus stimuli was accompanied by a reduction in the effect of spatial frequency (small-annulus: (t(1713)=−2.5, p = 0.014; large-annulus: (t(1713)=−2.5, p = 0.014). For the large annulus, there was also a reduction in the effect of temporal frequency (t(1713)=−2.1, p = 0.032).

There was also an interaction between the effects of spatial and temporal frequency (t(1713)=−3.1, p = 0.002). This was analysed in detail by evaluating the dependence of visual discomfort on spatial frequency separately for each temporal frequency, and the dependence on temporal frequency separately for each spatial frequency. The resulting slopes are shown in Fig. 8.

For static stimuli and those with a low flicker frequency, visual discomfort increased with spatial frequency. This effect of spatial frequency tended to decrease with increasing flicker rate, such that discomfort *decreased* with spatial frequency for the highest flicker frequency of 16 Hz. Discomfort increased with temporal frequency, with the slope of this relationship decreasing with spatial frequency. Overall, the greatest visual discomfort was evident when the highest flicker rates were combined with spatially uniform, or low spatial frequency stimuli.

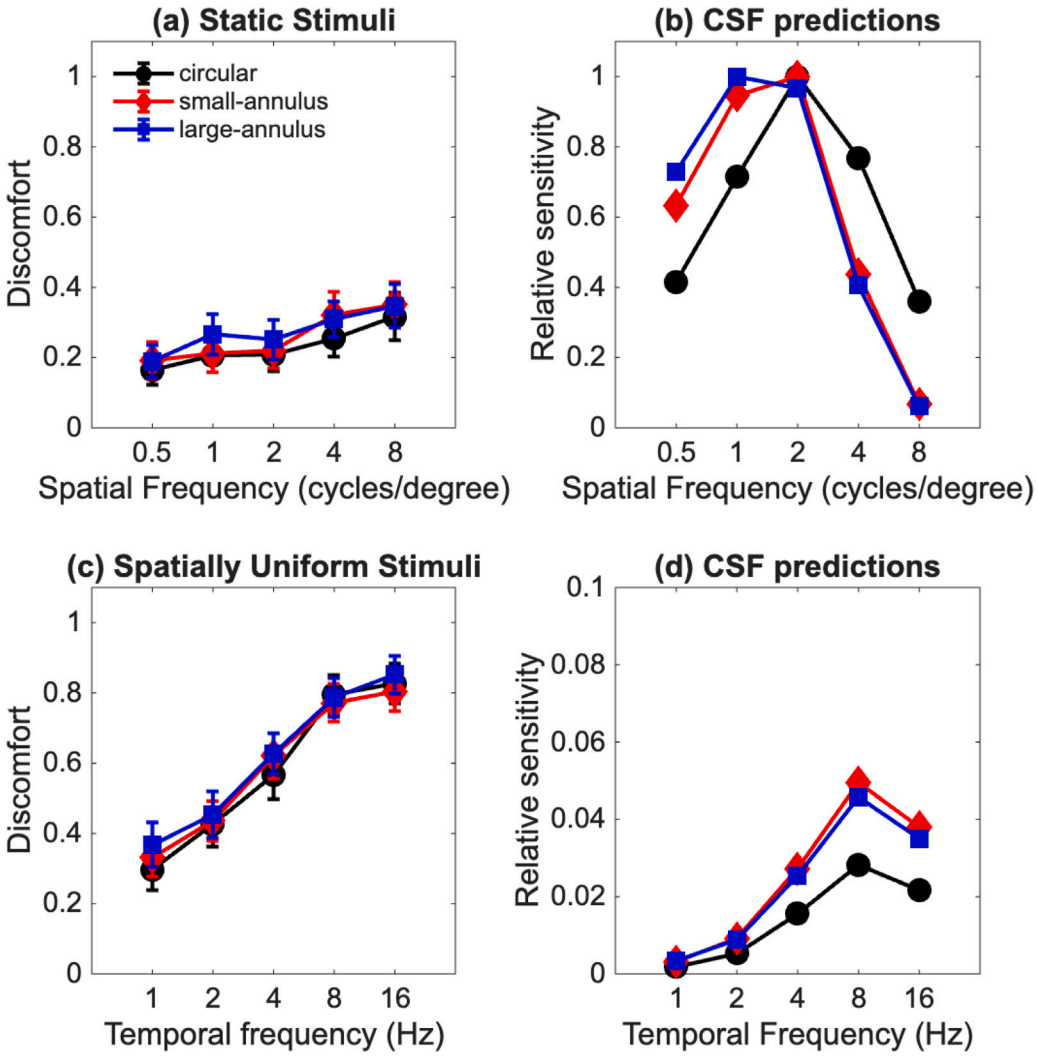

Fig. 4. (a) Mean discomfort ratings for static sinusoidal stimuli as a function of spatial frequency. Data are plotted separately for the circular stimuli and two sizes of annulus. (b) Predicted relative contrast sensitivity as a function of spatial frequency. Data are normalised against the maximum sensitivity across all stimuli (Ashraf et al., 2024). (c) Mean discomfort ratings for flickering, spatially uniform stimuli as a function of temporal frequency. (d) Predicted relative contrast sensitivity as a function of spatial frequency. Note the much reduced vertical axis range, used to show the temporal frequency tuning. Predicted contrast sensitivity is much lower for spatially uniform stimuli than for sinusoidal stripes. Error bars show ± 1 standard error of the mean.

3.4. Individual differences in sensory sensitivity and visual discomfort

For each participant, discomfort ratings were averaged across all conditions to obtain a single summary score, which was then correlated with the participant's Leiden Visual Sensory Sensitivity (L-VISS) total. The distribution of L-VISS scores across the sample are shown in Fig. 9a. There was a strong positive correlation between participants' L-VISS scores and average discomfort ratings ($r=0.59$, $p = 0.003$), as shown in Fig. 9b. Correlations were lower when only static images and pattern-related questions ($r=0.49$, $p = 0.017$), or unpatterned flicker and flicker-related questions ($r=0.21$; $p = 0.35$) were considered.

4. Discussion

4.1. Summary of main findings

The current study evaluated the influence of spatial and temporal frequency on discomfort for static and flickering sinusoidal stimuli, and for spatially uniform flicker. For static stimuli, discomfort increased with spatial frequency. For spatially uniform flickering stimuli, discomfort increased with temporal frequency. For flickering sinusoidal stimuli, there was an interaction between spatial and temporal frequency. At low flicker rates, discomfort increased with spatial frequency, but decreased with spatial frequency at the highest flicker rate of 16 Hz. Discomfort increased with flicker rate for all spatial frequencies. Discomfort was influenced more by flicker than by spatial frequency. Spatially uniform stimuli flickering at 16 Hz, the highest frequency tested, were rated as the most uncomfortable. The spatiotemporal tuning of visual discomfort was the same for central and peripheral stimuli.

4.2. Comparison with contrast sensitivity predictions

Our results are not consistent with the idea that visual discomfort reflects the CSF, either when considering the full spatio-temporal tuning, or each dimension individually. Peak contrast sensitivity is expected for static or slowly flickering stimuli (<2 Hz) with a midrange spatial frequency (2–4 cycles/degree), and to reduce for flicker rates of 16 Hz or higher. This contrasts with our finding that discomfort was maximum for rapidly flickering stimuli, particularly when these were spatially uniform.

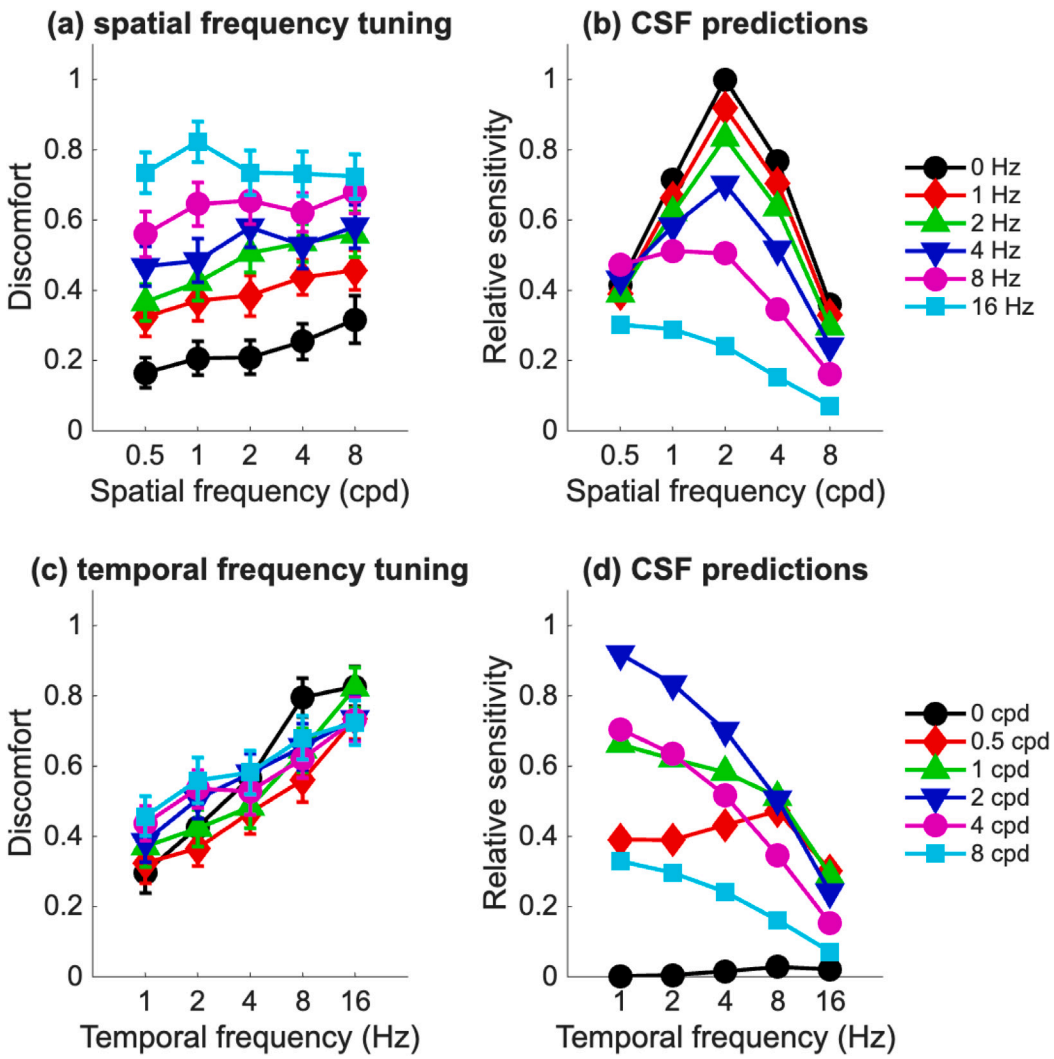

Fig. 5. Spatio-temporal discomfort tuning for the circular stimuli. (a) Discomfort as a function of spatial frequency plotted for each temporal frequency. (b) Predicted relative contrast sensitivity as a function of spatial frequency (Ashraf et al., 2024) (c) Discomfort as a function of temporal frequency plotted for each spatial frequency. (d) Predicted relative contrast sensitivity as a function of temporal frequency. Error bars show ± 1 standard error of the mean.

4.3. Stimulus range and apparatus constraints

It is possible, indeed likely, that discomfort would reduce for higher spatial and temporal frequencies than those used in the current study. However, the parameter ranges used (0–8 cycles/degree; 0–16 Hz) were chosen to bracket the expected peaks of the contrast sensitivity function (4 cycles/degree, 8 Hz). These values also approach the limits of the experimental apparatus used, with 5 pixels/cycle for the 8 cycles/degree patterns, and 7.5 frames per cycle for 16 Hz flicker. It would be interesting for future research to explore a broader parameter range, beyond that required to characterise the contrast sensitivity function.

4.4. Stimulus size and eccentricity

Our results were minimally affected by the manipulations of size and shape of the stimulus envelope. Again, this is inconsistent with predictions from the contrast sensitivity function, from which we expect bandpass spatial frequency tuning for our centrally presented circular stimuli, and a shift to more low-pass tuning for the peripherally presented annulus stimuli. It should be noted that, while participants were asked to maintain fixation, this was not monitored with eye-tracking, and it is possible that they might have made saccadic eye-movements, for example resulting in part of the annulus stimuli being fixated. While this is a limitation of the study, this possibility could not account for the mismatch between the discomfort ratings and the predictions of the contrast sensitivity function.

4.5. Individual differences and sensory sensitivity

It will also be interesting to explore individual differences in the spatio-temporal frequency tuning of visual discomfort. The participants in the current study were drawn from the general population, but there was a strong positive correlation between the average magnitude of discomfort ratings, and Leiden Visual Sensitivity Scale scores. A positive correlation of this kind is expected, since the L-VISS includes questions about responses to flicker and patterns, and participants were encouraged to interpret discomfort in the same terms. Nevertheless, it is reassuring to see a high correlation between subjective self-reflection, and immediate responses to the stimuli presented. A similarly high correlation has also been found between L-VISS scores and the Pattern Glare Test (Perenboom et al., 2018).

It is however of interest to consider why this value is not higher, given that the two approaches are measures of the same underlying phenomenon. This may be partly related to the difference between survey questions that measure traits (the extent to which individuals experience discomfort) and ratings that measure states (the experience

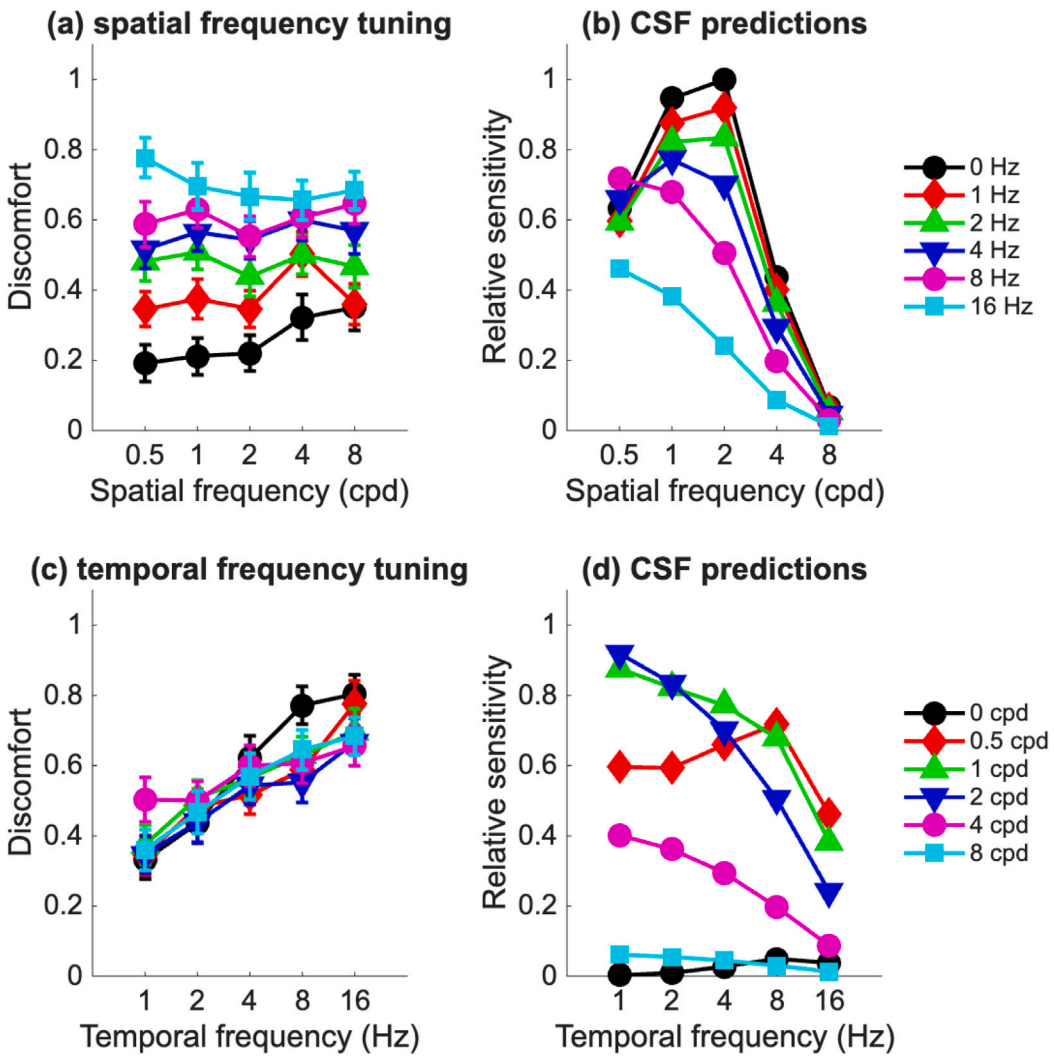

Fig. 6. Spatio-temporal discomfort tuning for the small-annulus stimuli. (a) Discomfort as a function of spatial frequency plotted for each temporal frequency. (b) Predicted relative contrast sensitivity as a function of spatial frequency (Ashraf et al., 2024) (c) Discomfort as a function of temporal frequency plotted for each spatial frequency. (d) Predicted relative contrast sensitivity as a function of temporal frequency. Error bars show ± 1 standard error of the mean.

of discomfort evoked by the current stimulus). Price et al. (2025) found higher correlations within survey measures than between survey and rating measures, and Burke et al. (in press) found higher correlations (r=.7) when only survey measures are used.

This difference in measurement types is exacerbated by the difficulty of calibrating the use of rating scales. Individual participants may be confident in using a rating scale to indicate differences in relative discomfort between stimuli, but there may be differences in how these scale values are used between people, especially given the wide variation in the severity of discomfort across the population. Anchoring techniques may be helpful in guiding how participants respond. Here, we directed participants to link their responses to the questions answered in the L-VISS, which includes experiences of viewing flicker and patterns. Price et al. (2025) used functional questions linked to aversion in a similar way. In addition, Clarke et al. (in revision) have proposed a two-stage technique that takes account of individual differences in the overall experience of discomfort when scaling responses.

While it would be interesting to investigate how the spatio-temporal frequency tuning of visual discomfort varies with sensory sensitivity, the current study did not target specific populations, and our sample is too small to be subdivided. However, other studies have found differences in spatial frequency tuning between groups. Conlon et al. (2001) compared discomfort ratings for static gratings for groups who were low, intermediate or high on the Visual Discomfort Scale (Conlon et al., 1999). For the low and intermediate groups, visual discomfort increased with spatial frequency from 1 to 12 cycles/degree. In contrast, for the high discomfort group, discomfort peaked at 4–8 cycles/degree, and reduced at 12 cycles/degree. Conlon et al.'s study is unique in measuring visual discomfort and contrast sensitivity for the same participants, and found differences between the two. Contrast sensitivity measures showed the expected peak at 2–4 cycles/degree for all groups, whereas discomfort peaked at 4–8 cycles/degree, or increased up to at least 12 cycles/degree, depending on the group. The stimuli that were rated as most uncomfortable were thus not the ones to which the visual system was most sensitive. Contrast sensitivity overall was lower for the high sensitivity group for static stimuli, but not for stimuli flickering at 6 Hz.

4.6. *Implications for neurophysiological measures*

It would also be interesting to expand the current study to include measurements of spatio-temporal contrast sensitivity, and visually evoked potentials and haemodynamic responses to the same stimuli that are rated for discomfort. This would allow direct comparison of individual differences in sensory sensitivity and cortical excitability with visual discomfort. The spatio-temporal inseparability of our results

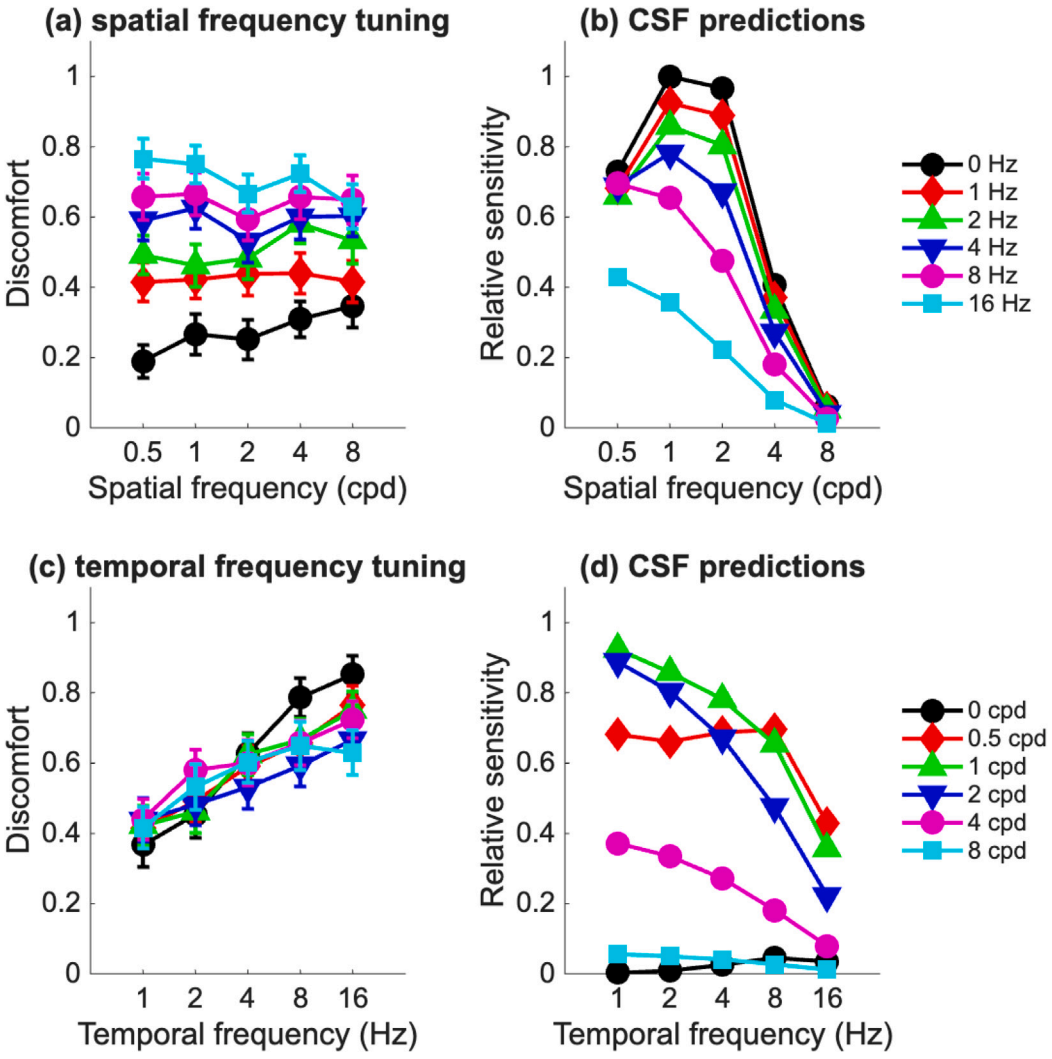

Fig. 7. Spatio-temporal discomfort tuning for the large stimuli. (a) Discomfort as a function of spatial frequency plotted for each temporal frequency. (b) Predicted relative contrast sensitivity as a function of spatial frequency (Ashraf et al., 2024) (c) Discomfort as a function of temporal frequency plotted for each spatial frequency. (d) Predicted relative contrast sensitivity as a function of temporal frequency. Error bars show ± 1 standard error of the mean.

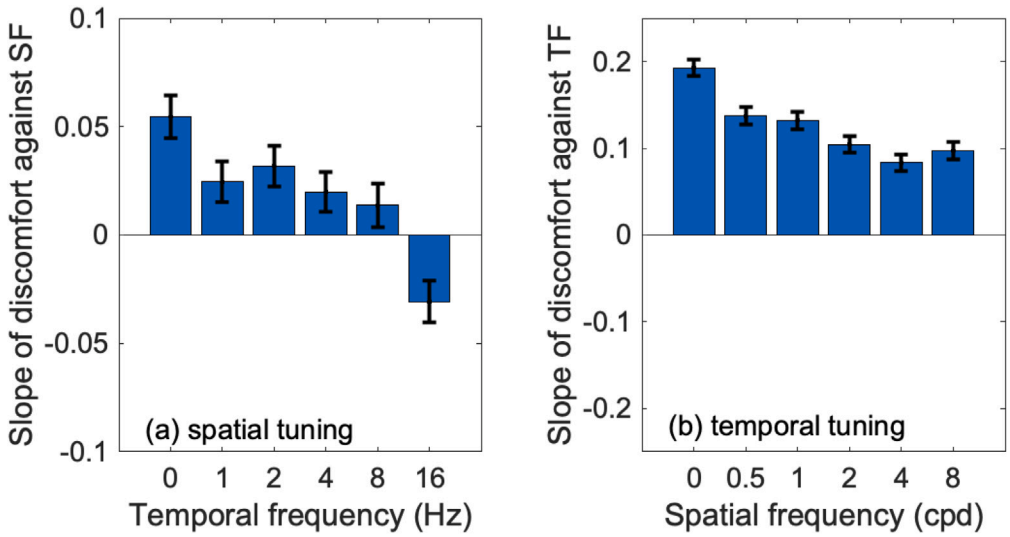

Fig. 8. (a) Slope of discomfort against spatial frequency as a function of temporal frequency. Discomfort increases with spatial frequency for stimuli with a low rate of flicker, but decreases with spatial frequency for stimuli with the highest rate of flicker (16 Hz). (b) Slope of discomfort against temporal frequency as a function of spatial frequency. Discomfort increases with temporal frequency in all cases. Error bars show ± standard error of the mean.

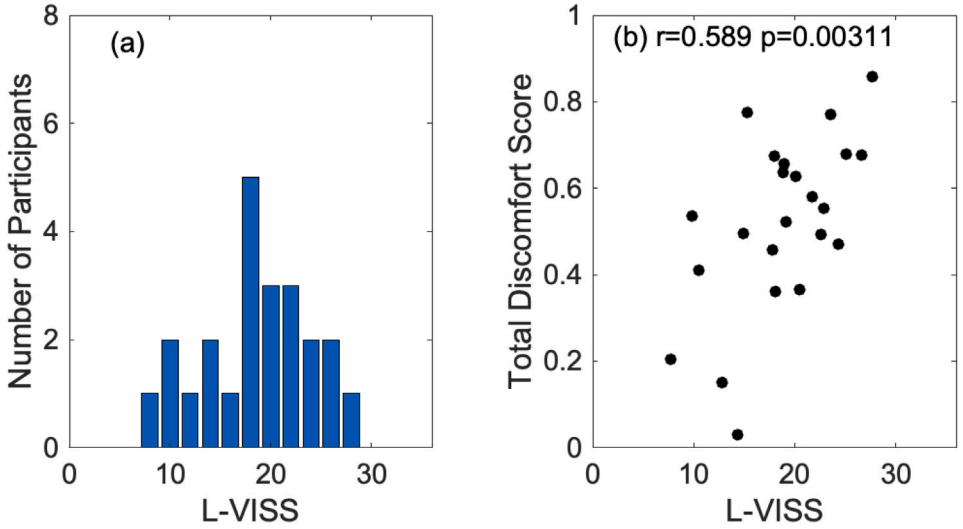

Fig. 9. (a) Distribution of the Leiden Visual Sensitivity (L-VISS) scores across participants (b) Scatterplot of L-VISS scores against mean discomfort ratings, showing a strong correlation between survey responses and stimulus ratings.

is a particularly pertinent consideration for methods such as steady-state visually evoked potentials, which depend on the presentation of flickering stimuli (Norcia et al., 2015). This highlights the need for multi-methods studies to use the same stimuli across different measurement types. For example, SSVEPs measured for flickering stimuli cannot be directly compared with visual discomfort ratings for static stimuli (O'Hare & Hibbard, 2024).

4.7. Factors underlying differences between studies

It remains unclear why the spatial frequency tuning of visual discomfort varies across studies (Conlon et al., 1999; Evans & Stevenson, 2008; Fernandez & Wilkins, 2008; Monger et al., 2016; O'Hare et al., 2015; O'Hare & Hibbard, 2011; Wilkins et al., 1984). A number of important factors differ between these studies. Firstly, a broad range of different stimuli have been used, including sinusoidal and squarewave gratings, filtered noise, artworks, and photographs. Secondly, these studies varied in their task requirements, some rating only discomfort, others comparing positive and negative ratings of pleasantness versus unpleasantness, and others reporting distortions and illusions. Thirdly, studies have varied in their participant groups, recruiting from the general public, distinguishing between low and high visual discomfort groups, or targeting particular populations with heightened sensory sensitivity, such as those with migraine (Perenboom et al., 2018; Shepherd, 2010)) or M.E. (Wilson et al., 2015).

4.8. Linking efficient coding models of contrast sensitivity to visual discomfort

The principles of efficient coding provide a potential explanation of the current results, and why the tuning of discomfort for spatial and temporal frequency might not reflect the CSF.

The bandpass spatial and temporal frequency tuning of the CSF can be explained by efficient encoding principles that take into account the statistical properties of natural visual stimuli (Atick & Redlich, 1992; Dong & Atick, 1995; Zhaoping, 2014). The Fourier amplitude of natural images reduces with both spatial and temporal frequency, such that the incoming signal is dominated by low frequency components in both dimensions. A process of decorrelation, in which the responses to the weaker, high frequency components is amplified, can be used to enhance the efficiency of neural encoding (Barlow et al., 1961). This however needs to be balanced with spatio-temporal smoothing of the signal to reduce the influence of noise.

These decorrelation and smoothing processes have opposite effects on signal encoding, as shown in Fig. 10. Filtering for decorrelation will increase the response with increasing frequency, so as to boost the weaker, high frequency signals. In contrast, smoothing will tend to reduce the response to high frequency components, where the signal-to-noise ratio is lowest. The bandpass tuning seen in the CSF has therefore been interpreted as a balance between the competing needs for decorrelation and noise reduction (Atick & Redlich, 1992; Dong & Atick, 1995).

At threshold levels of contrast, the signal-to-noise ratio will be relatively low. The lowpass and bandpass tuning found in the contrast sensitivity function are therefore consistent with the predictions of efficient coding principles (Figs. 10a and 10b) operating towards the lower end of the signal-to-noise range.

In an optimised system, the precise balance of whitening and smoothing will be determined by the signal-to-noise ratio of the stimulus (Fig. 10). This explains why contrast sensitivity shifts from bandpass to lowpass at low luminance levels (Atick & Redlich, 1992). In this case, the signal-to-noise ratio is reduced, and the effects of smoothing dominate over the effects of decorrelation.

At high contrast and high luminance, the signal-to-noise ratio will be at its maximum. This means that the effects of decorrelation will dominate, and responses will show high-pass tuning, increasing with frequency. This provides a potential explanation for the increase in visual discomfort with increasing spatial and temporal frequency found here. Assuming a high input signal-to-noise ratio, efficient coding principles predict that the response gain would be highest for high spatial and temporal frequencies, since they tend to have a low amplitude in natural scenes. This high gain, when applied to unexpectedly high contrast high frequency content relative to natural images, could then account for high discomfort via hyperexcitation.

Our results are consistent with some physiological measures of cortical responses to high contrast stimuli that show the highest responses to higher spatial and temporal frequencies than are found for threshold level contrast sensitivity measures (Gentile & Aguirre, 2020; Norcia et al., 2015; Spitschan et al., 2016; Tyler et al., 1979).

This efficient encoding might also be able to explain the individual differences found in some studies. If higher susceptibility to visual discomfort is associated with greater levels of cortical noise, as for example found in migraine (O'Hare et al., 2025), this would explain why maximum discomfort occurs at a lower spatial frequency (Conlon et al., 2001), due to an increase in the influence of spatial smoothing relative to decorrelation.

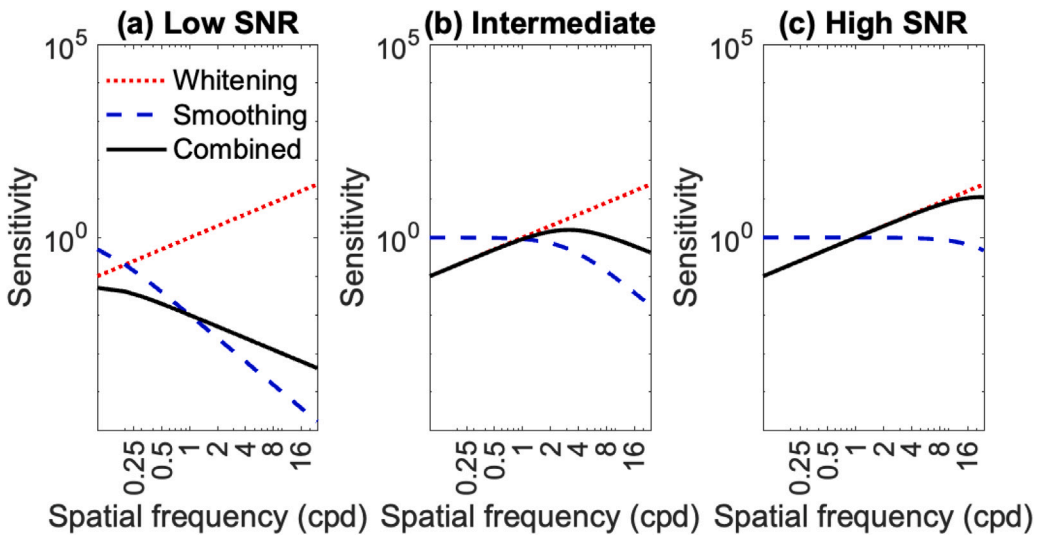

Fig. 10. Efficient encoding filters balance the need for gain control via decorrelation, or whitening (red curve), to equalise the signal response across frequencies, and smoothing (blue curve), to reduce the effects of noise. The overall response (black curve) shows the joint effect of the whitening and smoothing filters. The degree of smoothing required varies with signal-to-noise ratio. (a) With a low signal-to-noise ratio, smoothing is strongly low-pass, leading to an overall low-pass response. (b) At an intermediate signal-to-noise ratio, less smoothing is required, and the overall response is bandpass. (c) With a high signal-to-noise ratio, smoothing only affects the very highest spatial frequencies, and the overall response is high-pass across the frequency range shown.

4.9. Conclusion

This study presents the first comprehensive mapping of spatio-temporal tuning for visual discomfort. Discomfort increased with spatial frequency for static and slowly flickering stimuli, but decreased with spatial frequency for stimuli flickering at 16 Hz. For spatially uniform stimuli, and for all patterned stimuli, discomfort increased with temporal frequency, with 16 Hz spatially uniform flicker rated as most uncomfortable overall. Temporal frequency had a stronger influence on discomfort than spatial frequency, and the observed tuning patterns diverged from those predicted by the contrast sensitivity function. These findings suggest that visual sensitivity at threshold does not reliably predict discomfort for high-contrast stimuli. The difference in the relative influence of smoothing and decorrelation mechanisms between low and high contrast stimuli provides a potential explanation for the difference between the CSF and the tuning of visual discomfort for high contrast stimuli.

CRediT authorship contribution statement

Paul B. Hibbard: Writing – original draft, Visualization, Validation, Supervision, Software, Project administration, Methodology, Data curation, Conceptualization. **Jordi M. Asher:** Writing – original draft, Visualization, Supervision, Software, Project administration, Methodology, Conceptualization. **Louise O'Hare:** Writing – review & editing, Conceptualization. **Caitlin Evans:** Writing – review & editing, Investigation, Data curation, Conceptualization. **Caelan Dow:** Writing – review & editing, Investigation, Data curation, Conceptualization.

References

Ashraf, M., Mantiuk, R. K., Chapiro, A., & Wuerger, S. (2024). castleCSF—A contrast sensitivity function of color, area, spatiotemporal frequency, luminance and eccentricity. *Journal of Vision*, *24*(4), 5.

Atick, J. J., & Redlich, A. N. (1992). What does the retina know about natural scenes? *Neural Computation*, *4*(2), 196–210.

Barlow, H. B., et al. (1961). Possible principles underlying the transformation of sensory messages. *Sensory Communication*, *1*(01), 217–233.

Brainard, D. H., Kleiner, M., Pelli, D. G., Ingling, A., et al. (2024). Psychtoolbox: Software for visual psychophysics and neuroscience experiments. *Journal of Vision*, *24*(2), 1–17.

Conlon, E., Lovegrove, W., Barker, S., & Chekaluk, E. (2001). Visual discomfort: the influence of spatial frequency. *Perception*, *30*(5), 571–581.

Conlon, E. G., Lovegrove, W. J., Chekaluk, E., & Pattison, P. E. (1999). Measuring visual discomfort. *Visual Cognition*, *6*(6), 637–663.

Dong, D. W., & Atick, J. J. (1995). Temporal decorrelation: a theory of lagged and nonlagged responses in the lateral geniculate nucleus. *Network: Computation in Neural Systems*, *6*(2), 159.

Evans, B., & Stevenson, S. (2008). The pattern glare test: a review and determination of normative values. *Ophthalmic & Physiological Optics*, *28*(4), 295–309.

Fernandez, D., & Wilkins, A. J. (2008). Uncomfortable images in art and nature. *Perception*, *37*(7), 1098–1113.

Gentile, C. P., & Aguirre, G. K. (2020). A neural correlate of visual discomfort from flicker. *Journal of Vision*, *20*(7), 11.

Haigh, S. M., Barningham, L., Berntsen, M., Coutts, L. V., Hobbs, E. S., Irabor, J., Lever, E. M., Tang, P., & Wilkins, A. J. (2013). Discomfort and the cortical haemodynamic response to coloured gratings. *Vision Research*, *89*, 47–53.

Hibbard, P. B., & O'Hare, L. (2015). Uncomfortable images produce non-sparse responses in a model of primary visual cortex. *Royal Society Open Science*, *2*(2), Article 140535.

Huang, J., Cooper, T. G., Satana, B., Kaufman, D. I., & Cao, Y. (2003). Visual distortion provoked by a stimulus in migraine associated with hyperneuronal activity. *Headache: The Journal of Head and Face Pain*, *43*(6), 664–671.

Huang, J., Zong, X., Wilkins, A., Jenkins, B., Bozoki, A., & Cao, Y. (2011). fMRI evidence that precision ophthalmic tints reduce cortical hyperactivation in migraine. *Cephalalgia*, *31*(8), 925–936.

Kleiner, M., Brainard, D., Pelli, D., Ingling, A., Murray, R., & Broussard, C. (2007). What's new in psychtoolbox-3. *Perception*, *36*(14), 1–16.

Kurczewska, E., Ferensztajn-Rochowiak, E., Rybakowski, J., & Rybakowski, F. (2024). Sensory processing sensitivity as a trait of temperament - evolutionary, socio-cultural, biological context and relation to mental disorders. *Psychiatria Polska*, *58*(2), 249–264.

Legge, G. E. (1978). Sustained and transient mechanisms in human vision: Temporal and spatial properties. *Vision Research*, *18*(1), 69–81.

Masri, R. A., Grünert, U., & Martin, P. R. (2020). Analysis of parvocellular and magnocellular visual pathways in human retina. *Journal of Neuroscience*, *40*(42), 8132–8148.

Monger, L. J., Shah, D., Wilkins, A. J., & Allen, P. M. (2016). The effect of viewing distance on responses to the pattern glare test. *Clinical and Experimental Optometry*, *99*(1), 47–50.

Norcia, A. M., Appelbaum, L. G., Ales, J. M., Cottereau, B. R., & Rossion, B. (2015). The steady-state visual evoked potential in vision research: a review. *Journal of Vision*, *15*(6), 4.

Ogawa, N., & Motoyoshi, I. (2021). Spatiotemporal frequency characteristics of the visual unpleasantness of dynamic bandpass noise. *Vision Research*, *184*, 37–42.

O'Hare, L. (2017). Steady-state VEP responses to uncomfortable stimuli. *European Journal of Neuroscience*, *45*(3), 410–422.

O'Hare, L., Clarke, A. D., & Pollux, P. M. (2015). VEP responses to op-art stimuli. *PLoS One*, *10*(9), Article e0139400.

O'Hare, L., & Hibbard, P. B. (2011). Spatial frequency and visual discomfort. *Vision Research*, *51*(15), 1767–1777.
O'Hare, L., & Hibbard, P. B. (2024). Support for the efficient coding account of visual discomfort. *Visual Neuroscience*, *41*, E008.
O'Hare, L., Hibbard, P. B., & Wilkins, A. J. (2025). Evidence for increased background neural noise in migraine with aura: hyperactive but not hyperresponsive. *Headache*, *00*, 1–18.
Orekhova, E. V., Stroganova, T. A., Schneiderman, J. F., Lundström, S., Riaz, B., Sarovic, D., Sysoeva, O. V., Brant, G., Gillberg, C., & Hadjikhani, N. (2019). Neural gain control measured through cortical gamma oscillations is associated with sensory sensitivity. *Human Brain Mapping*, *40*(5), 1583–1593.
Penacchio, O., Otazu, X., Wilkins, A. J., & Haigh, S. M. (2023). A mechanistic account of visual discomfort. *Frontiers in Neuroscience*, *17*.
Perenboom, M. J., Najafabadi, A. H. Z., Zielman, R., Carpay, J. A., & Ferrari, M. D. (2018). Quantifying visual allodynia across migraine subtypes: the leiden visual sensitivity scale. *Pain*, *159*(11), 2375–2382.
Price, A., Powell, G., & Sumner, P. (2025). Low correlation between visual discomfort image ratings and hypersensitivity questions is improved with functional questions. *Vision Research*, *228*, Article 108551.
Price, A., Sumner, P., & Powell, G. (2025a). The subtypes of visual hypersensitivity are transdiagnostic across neurodivergence, neurology and mental health. *Vision Research*, *234*, Article 108640.
Price, A., Sumner, P., & Powell, G. (2025b). Understanding the subtypes of visual hypersensitivity: Four coherent factors and their measurement with the Cardiff hypersensitivity scale (CHYPS). *Vision Research*, *233*, Article 108610.
Regan, D. (1978). Assessment of visual acuity by evoked potential recording: ambiguity caused by temporal dependence of spatial frequency selectivity. *Vision Research*, *18*(4), 439–443.
Regan, D. (1989). *Evoked Potentials and Evoked Magnetic Fields in Science and Medicine*. New York: Elsevier.
Robson, J. G. (1966). Spatial and temporal contrast-sensitivity functions of the visual system. *Journal of the Optical Society of America*, *56*(8), 1141–1142.
Schiller, P. H., & Logothetis, N. K. (1990). The color-opponent and broad-band channels of the primate visual system. *Trends in Neurosciences*, *13*(10), 392–398.
Shepherd, A. J. (2010). Visual stimuli, light and lighting are common triggers of migraine and headache. *Journal of Light & Visual Environment*, *34*(2), 94–100.
Shepherd, A. J., Hine, T. J., & Beaumont, H. M. (2013). Color and spatial frequency are related to visual pattern sensitivity in migraine. *Headache: The Journal of Head and Face Pain*, *53*(7), 1087–1103.
Spitschan, M., Datta, R., Stern, A. M., Brainard, D. H., & Aguirre, G. K. (2016). Human visual cortex responses to rapid cone and melanopsin-directed flicker. *Journal of Neuroscience*, *36*(5), 1471–1482.
Strasburger, H., Rentschler, I., & Jüttner, M. (2011). Peripheral vision and pattern recognition: A review. *Journal of Vision*, *11*(5), 13.
Tyler, C. W., Apkarian, P., Levi, D. M., & Nakayama, K. (1979). Rapid assessment of visual function: an electronic sweep technique for the pattern visual evoked potential. *Investigative Ophthalmology & Visual Science*, *18*(7), 703–713.
Tyler, C., Apkarian, P., & Nakayama, K. (1978). Multiple spatial-frequency tuning of electrical responses from human visual cortex. *Experimental Brain Research*, *33*(3), 535–550.
Ward, J. (2019). Individual differences in sensory sensitivity: A synthesizing framework and evidence from normal variation and developmental conditions. *Cognitive Neuroscience*, *10*(3), 139–157.
Wilkins, A. J. (1995). *Visual Stress*. OUP Oxford.
Wilkins, A. J., & Hibbard, P. B. (2014). Discomfort and hypermetabolism. In *Presented at AISB 2014 - 50th annual convention of the AISB*.
Wilkins, A., Nimmo-Smith, I., Tait, A., McManus, C., Della Sala, S., Tilley, A., Arnold, K., Barrie, M., & Scott, S. (1984). A neurological basis for visual discomfort. *Brain*, *107*(4), 989–1017.
Wilson, R. L., Paterson, K. B., & Hutchinson, C. V. (2015). Increased vulnerability to pattern-related visual stress in myalgic encephalomyelitis. *Perception*, *44*(12), 1422–1426.
Yoshimoto, S., Garcia, J., Jiang, F., Wilkins, A. J., Takeuchi, T., & Webster, M. A. (2017). Visual discomfort and flicker. *Vision Research*, *138*, 18–28.
Zhaoping, L. (2014). *Understanding Vision: Theory, Models, and Data*. Oxford University Press.